Chapter 4

Vesicular Self-assembly of Crotocembraneic Acid

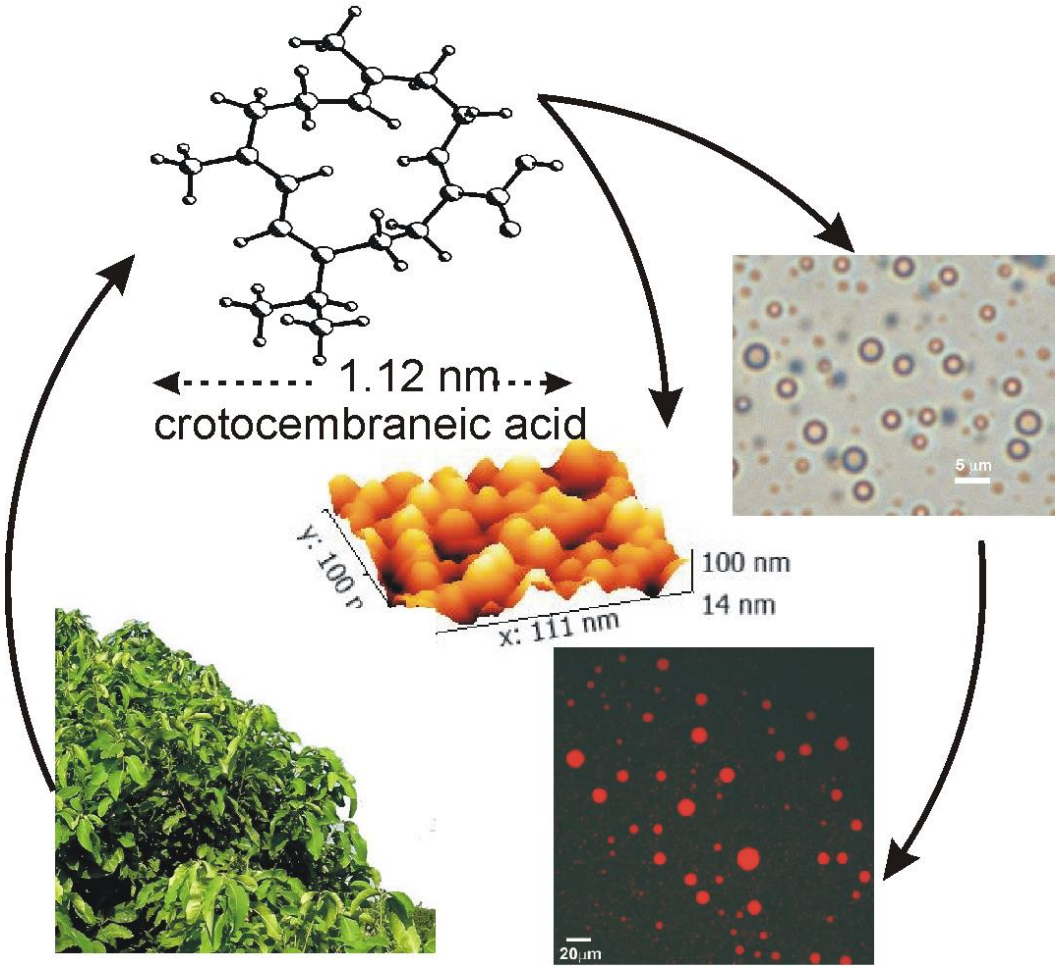

4.1 Introduction

Spontaneous hierarchical self-assembly of small molecules in liquids yielding self-assemblies of nano- to micro-meter dimensions such as vesicles, fibers, spheres, tubules, etc. has become an area of intense research in recent years for an improved understanding of the structure property relationships and because of their many potential and realized technological applications.[1,2,3,4,5,6] Studies of the vesicular self-assembly of small molecules in aqueous binary solvent mixtures are of special interest because of its tremendous applications in the areas of controlled-release drug delivery systems, medical implants, tissue engineering, etc.[7,8] Literature study reveals that majority of the examples having the aforementioned applications are

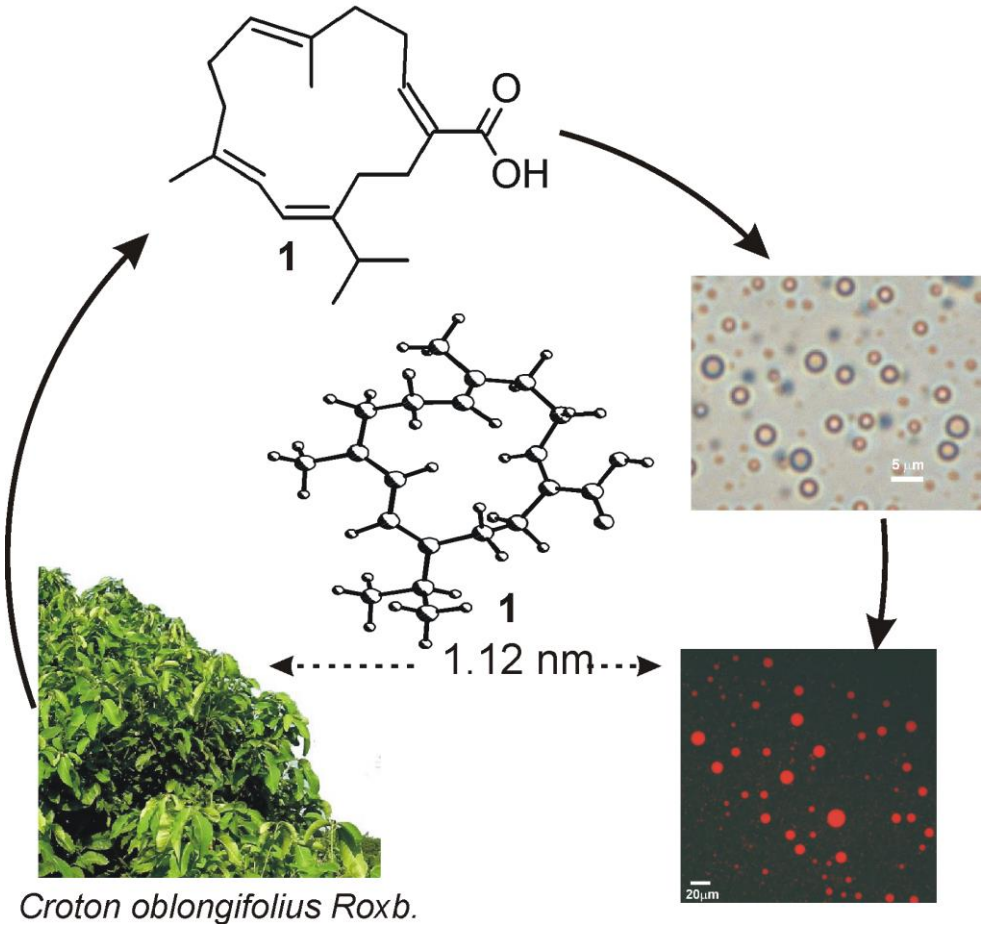

Figure 1: Schematic representation of self-assembly of crotocembraneic acid **1** extractable from Croton oblongifolius Roxb yielding vesicular selfassemblies and its use in drug entrapment studies (centre: energy minimized structure of **1**).

based upon low molecular weight organic compounds that are often obtained either by multistep chemical synthesis or polymeric systems that are capable of gelling aqueous solvent mixtures.[9,10,11,12] Self-assemblies of molecules from renewable resources are of great significance in recent years because their availability in renewable supply, low toxicity and biodegradability will aid to establish a sustainable society.[13] But, vesicular self-assemblies of molecules from renewable resources in aqueous solvent mixtures are rare.[14,15]

Recently we have reported the spontaneous hierarchical self-assembly of two triterpenic acids and their derivatives that yielded vesicular self-assemblies.[14,16] But, according to our knowledge, there is no report in the literature on the spontaneous self-assembly of naturally occurring diterpenoids. In continuation of our investigations on the utilization of terpenoids as renewables,[17,18,19] herein we report the first self-assembly properties of a nano-sized macrocyclic diterpenoid crotocembraneic acid 1 (Figure 1) in different liquids. The diterpenoid extractable from *Croton oblongifolius* Roxb. spontaneously self-assembled in aqueous binary solvent mixtures yielding vesicular self-assemblies of nano to micrometer diameters. The self-assemblies were capable of entrapping various fluorophores including the anticancer drug doxorubicin making it useful for targeted drug delivery applications. Crotocembraneic acid **1** was extracted from the leaves of Croton oblongifolius Roxb. as a low melting solid following an optimized procedure developed in our laboratory. The molecule has a unique 14-membered macrocyclic structure having four double bonds within the macrocycle with two of them in conjugated and two in the non-conjugated positions. The length of the molecule, obtained by molecular mechanics calculation using Allinger's MMX algorithm, was 1.12 nm (Figure 1 and Figure 2). The carboxyl group forming a polar head group and the macrocycle

forming a highly hydrophobic tail, crotocembraneic acid **1** turned out to be a unique macrocyclic amphiphile for the study of its self-assembly properties in various liquids.[20]

4.2 Results and Discussions

4.2.1 Plant material

Leaves of *C. oblongifolius* were collected from Nakhonsawan province, Thailand, in October 2014. The plant, *C. oblongifolius*, was previously authenticated by Panarat Charoenchai, and the specimen (no. CRI 285) was deposited at the Laboratory of Natural Products, Chulabhorn Research Institute.[1]

4.2.2 Isolation and Purification of crotocembraneic acid

Powdered, air-dried leaves (0.8 kg) of *C. oblongifolius* were macerated with CH_2Cl_2 to yield a crude extract of 37.6 g. The crude extract was subjected to silica gel column chromatography (CC) (10×56 cm), eluted with hexane:CH_2Cl_2 (8:2) and CH_2Cl_2:MeOH (9:1) stepwise gradients, to yield nineteen fractions (A1 to A19). Fraction A11 (1.37 g) was separated by Sephadex LH-20 CC (3x100 cm) eluted with MeOH to obtain eleven fractions (B1-B11). Fractions B10 and B11 which had similar TLC patterns and ^{1}H NMR spectra were combined (395.0 mg) and further separated by silica gel CC (1.5×17 cm), eluted with a gradient solvent system of hexane:CH_2Cl_2 (4:6) to yield crotocembraneic acid **1** (77.7 mg). Similarly, fractions A12-A14 which had similar TLC patterns and ^{1}H NMR spectra were combined (2.12 g) and further separated by silica gel Sephadex LH-20 CC (3x100 cm) eluted with MeOH to obtain seventeen fractions (C1-C17). Fractions C10-C13 (1.20 g) were combined and further separated using Sephadex LH-20 CC (2x122 cm) eluted with MeOH:CH_2Cl_2 (1:3) to yield crotocembraneic acid **1** (654.0 mg). Fraction A15 and A16 which had similar TLC patterns and ^{1}H NMR spectra were combined (4.26

g) and further separated by silica gel Sephadex LH-20 CC (3x100 cm) eluted with MeOH giving crotocembraneic acid **1** (1.56 g).

Table 1 ^{1}H (300 MHz) and ^{13}C NMR (75 MHz) data of crotocembraneic acid (**1**) in $CDCl_3$

	Crotocembraneic acid **1**	
Position	δ_C (ppm)	δ_H (ppm), (*J* in Hz)
1	146.3	-
2	118.7	6.04 (d, *J* = 10.5)
3	121.6	5.87 (d, *J* = 11.3)
4	135.2	-
5	39.2	2.14 (m)
6	25.1	2.20 (m)
7	125.7	5.11 (t, *J* = 5.9)
8	134.0	-
9	38.5	2.16 (m)
10	26.4	2.71 (m)
11	146.6	6.01 (t, *J* = 5.2)
12	130.9	-
13	28.7	2.36 (m)
14	33.6	2.41 (m)
15	33.7	2.34 (m)
16	22.1	1.02 (d, *J* = 6.8)
17	22.1	1.02 (d, *J* = 6.8)
18	17.0	1.74 (s)
19	15.8	1.55 (s)
20	173.6	-

Spectroscopic data of crotocembraneic acid (**1**) were in good agreement with those published in the literature.[2]

4.2.3 Properties of crotocembraneic acid 1

White crystals; UV (EtOH) λ_{max} (log ε): 204.0 (3.39) nm; IR (UATR) ν_{max} 3422, 2957, 2927, 1712, 1454, 1377, 1180, 1059, 736, 703 cm^{-1}; HRESI-MS: *m/z* 303.2314 $(M+H)^+$, calcd *m/z* 303.2311 for $C_{20}H_{31}O_6$; ^1H and ^{13}C NMR spectroscopic data, see Table 2

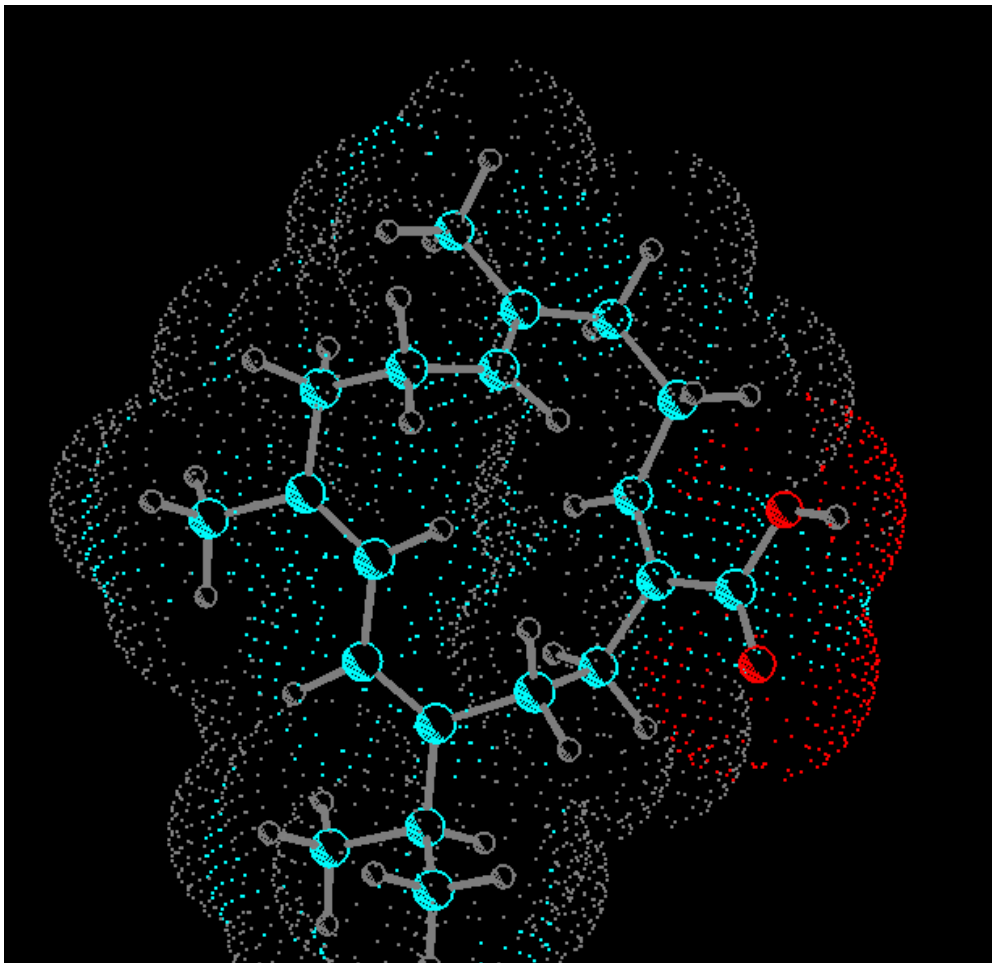

Figure 2: Energy minimized structure of Crotocembraneic acid (**1**) (PCWin,® Serena Software, version 9.2). The amphiphilic nature of the molecule with the polar carboxyl 'head' group and macrocyclic 'lypophilic' backbone is depicted.

4.2.4 Self-assembly study

Compound 1 was highly soluble in polar solvents such as ethanol, DMSO, DMF. When a hot and stirred solution of 1 in DMSO (100 μL) contained in a vial was

treated with water (50 □L) and the resulting mixture was allowed to cool at room temperature, a colloidal suspension was obtained in 15 min. Such colloidal suspensions were also obtained in DMF-water and ethanol-water mixtures (Table 1).

Table 2. Self-assembly crotocembraneic acid **1** in aqueous binary solvent mixtures

Entry	**Solvent**[a]	**Conc. (% w/v)**	**State**[b]
1	ethanol-water	2	CS
2	DMSO-water	2	CS
3	DMF-water	2	CS

[a] solvent : water in 2:1 v/v ratio, CS = colloidal suspension

4.2.5 Morphology Studies

The morphology of the self-assemblies were studied by atomic force microscopy (AFM), scanning electron microscopy (SEM), high resolution transmission electron microscopy (HRTEM), optical microscopy, dynamic light scattering (DLS), FTIR and XRD studies.

4.2.5.1 Optical microscopy and scanning electron microscopy

Optical microscopy (OM) of a colloidal suspension of **1** (2% w/v) in ethanol-water (2:1 v/v), DMSO-water (2:1 v/v) and DMF-water (2:1 v/v) indicated micro-sized spherical self-assemblies of average diameter of 2 μm (Figure 3,a-c and Figure 5). The nano-sized self-assemblies could not be observed by OM due to limitation of the technique used. This limitation was overcome by scanning electron microscopy.

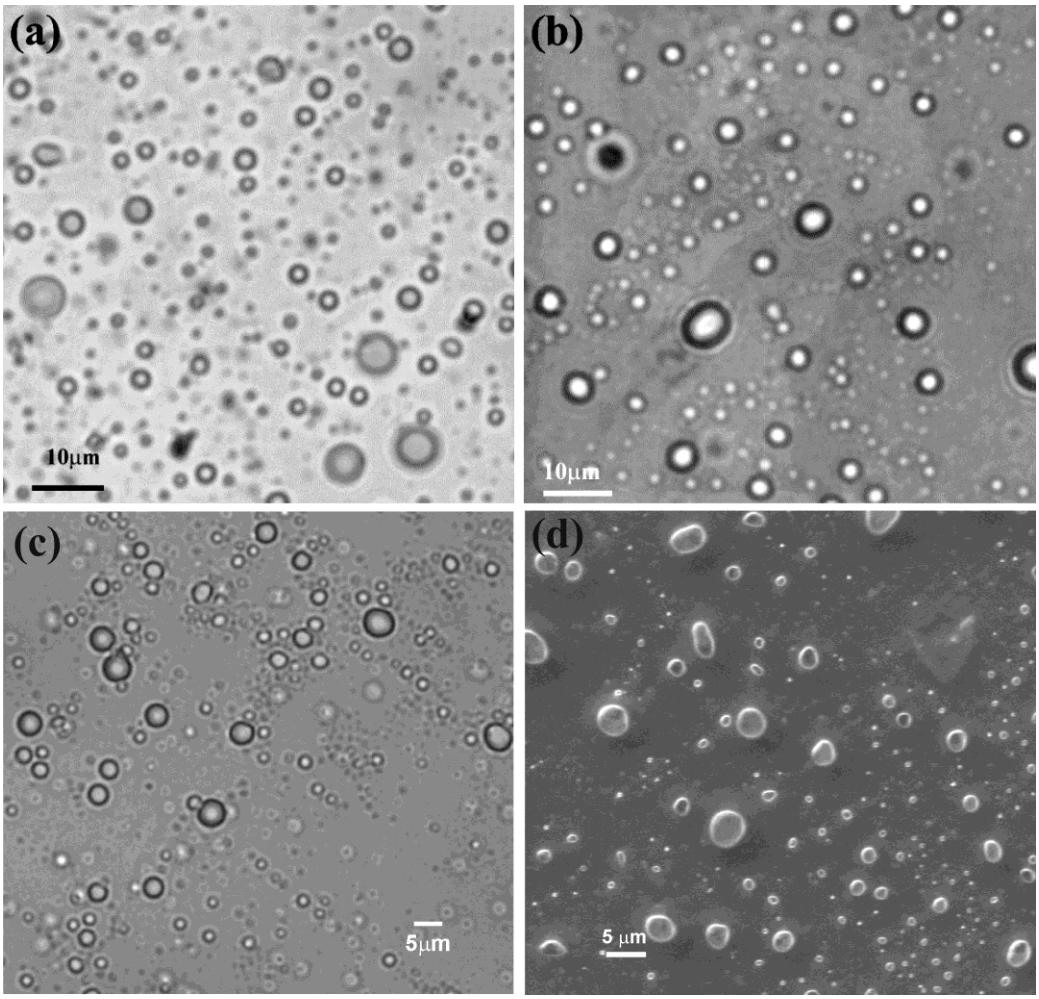

Figure 3: (a-c) Optical micrographs of Crotocembraneic acid **1** in (a) ethanol-water (2% w/v) (b) DMSO-water (2% w/v) (c) DMF-water (2% w/v); (d) SEM of **1** (0.28% w/v) in DMSO-water (2:1 v/v).

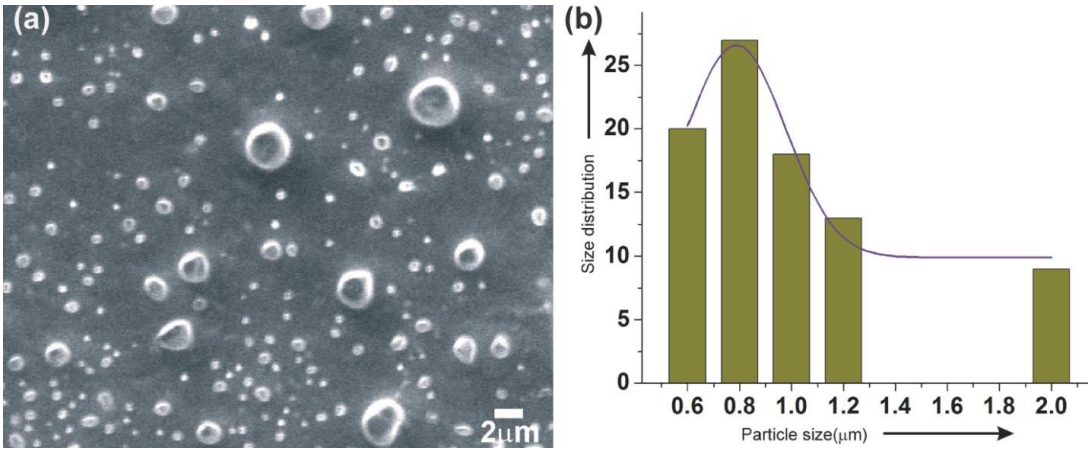

Figure 4: SEM images of a dry sample prepared from crotocembraneic acid 1 in DMSO-water (2:1, v/v) (0.28% w/v) (a) Spheres (diameter = 780 nm); b) histogram

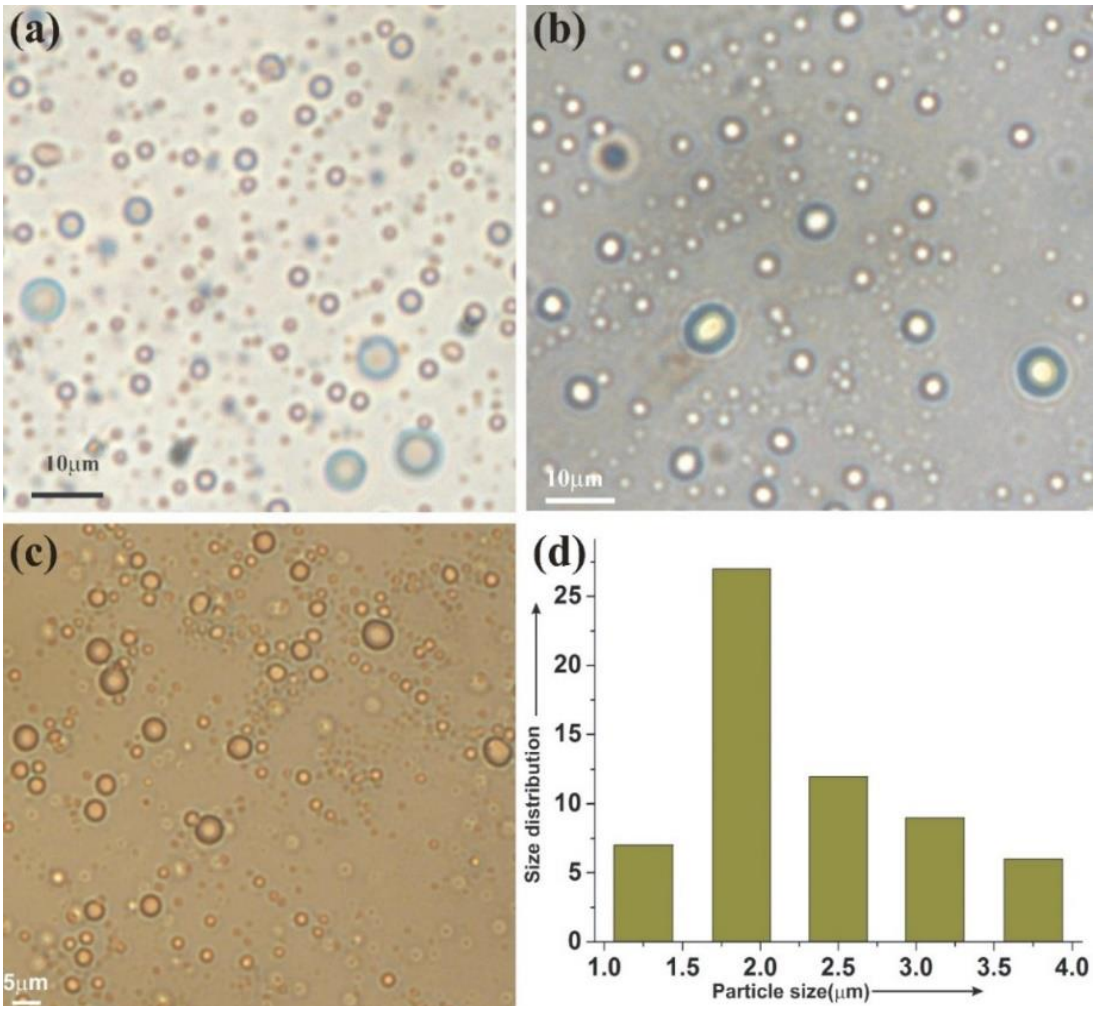

Figure 5: Polarizing optical micrographs (recorded in NIKON ECLIPSE LV100POL instrument) of Crotocembraneic acid in (a) Ethanol-water (2%w/v) (b) DMSO-Water (2%w/v) (c) DMF-Water (2%w/v) (d) histogram

For example, when the dried self-assemblies of **1** prepared from its colloidal suspension in DMSO-water (0.28% w/v) was examined by SEM (basic), the presence of both nano as well as micrometer sized spherical self-assemblies (Figure 3d and Figure 4) were observed. Field emission scanning electron microscopy (FESEM) of the dried self-assemblies of **1** revealed spherical self-assemblies of average size of 30 nm (Figure 6a).

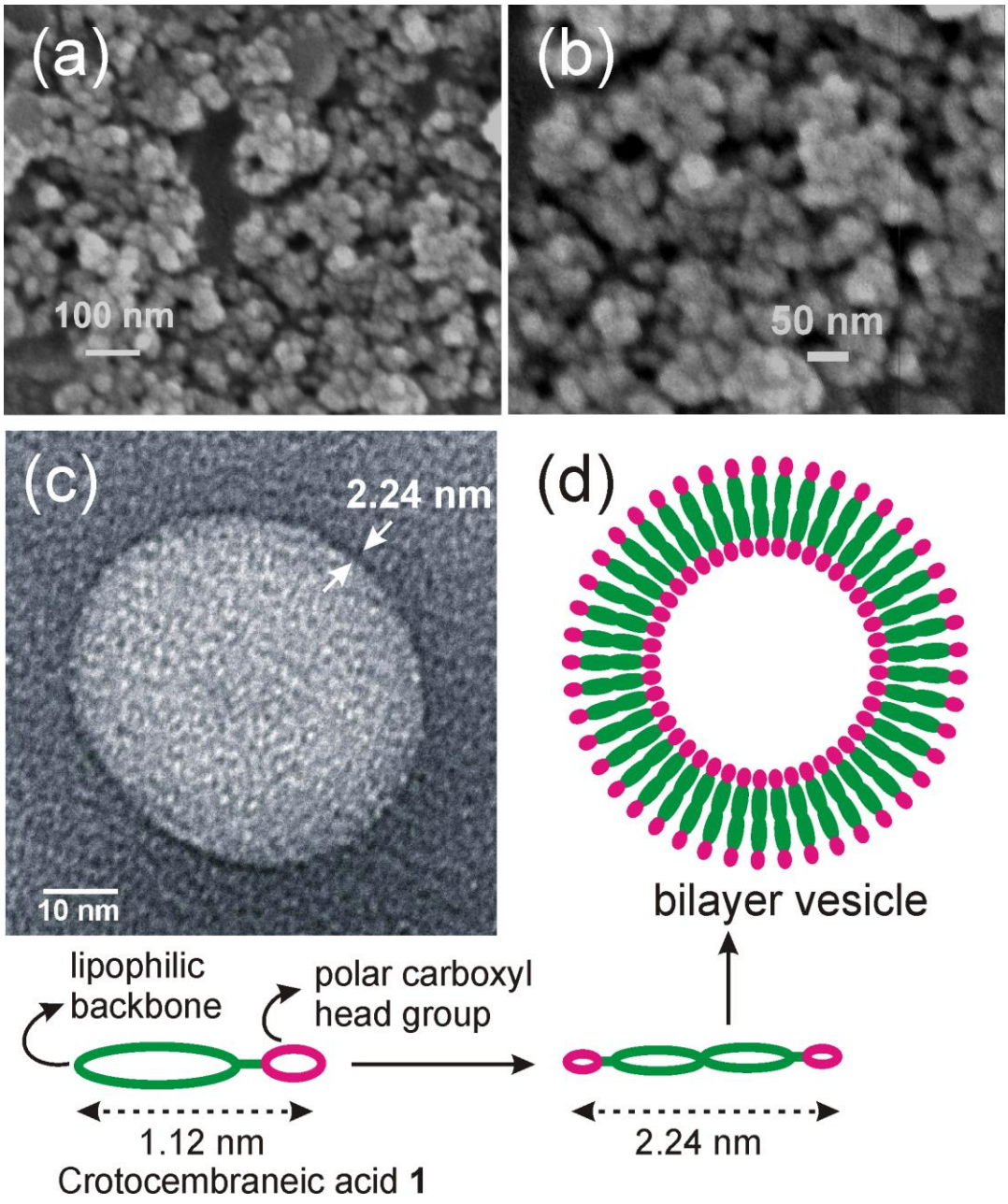

Figure 6: (a,b) FESEM of dried self-assemblies of 1 (0.28% w/v) prepared from its colloidal suspension in DMSO-water (2:1 v/v), (c) HRTEM of dried self-assemblies of **1** prepared from its colloidal suspension in ethanol-water (2:1 v/v), (d) schematic representation of the formation of bilayer membrane yielding vesicular self-assembly of **1.**

4.2.5.2 HRTEM Studies

To get further insight of the nature of the spherical self-assemblies, a dried sample prepared from the self-assemblies of **1** (0.28% w/v) in ethanol-water (2:1 v/v) was

analyzed by High Resolution Transmission Electron Microscopy (HRTEM). Spherical self-assemblies with distinct periphery having a membrane structure indicated the vesicular nature of the spheres. With a membrane thickness of 2.24 nm and the molecular length being 1.12 nm, a bilayer vesicular self-assembly is supported (Figure 6c). Fusion of smaller sized vesicles yielding bigger vesicles has also been observed by HRTEM (Figure 7).

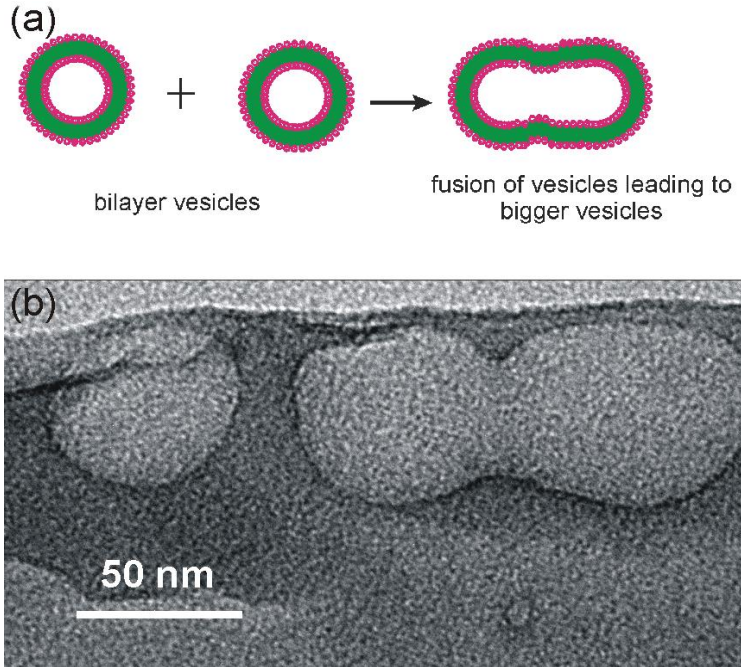

Figure 7: (a) schematic representation of fusion of two vesicles forming a bigger vesicle, (b) HRTEM image showing fused vesicle

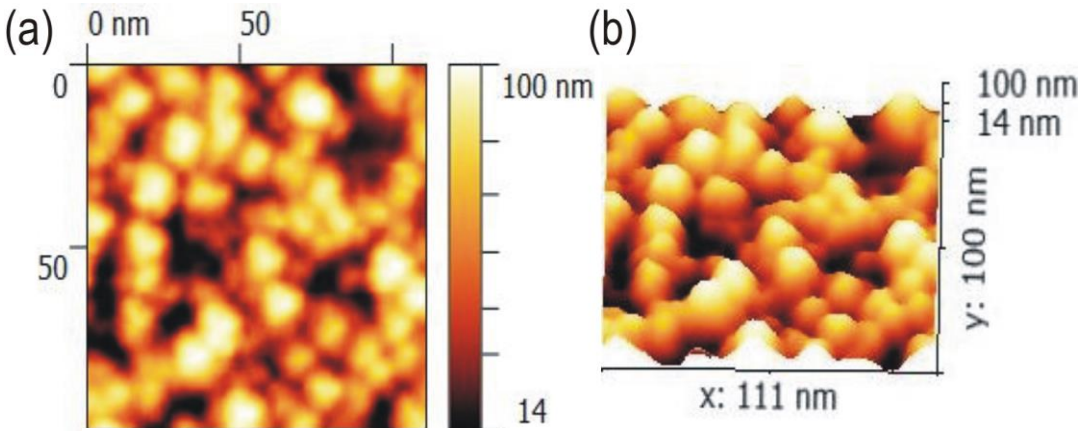

Figure 8: (a,b) AFM images (2D and 3D respectively) of spherical self-assemblies formed from **1** (0.28% w/v) in DMSO-water (2:1 v/v).

4.2.5.3 Atomic Force Microscopy

Atomic force microscopy of a dried sample prepared from a colloidal suspension of 1 (0.28% w/v) in DMSO-water (2:1 v/v) revealed spherical self-assemblies of 40-50 nm diameters (Figure 8 and Figure 9). The measured heights of the spherical self-assemblies were smaller than the diameters indicating the soft nature of the assemblies.

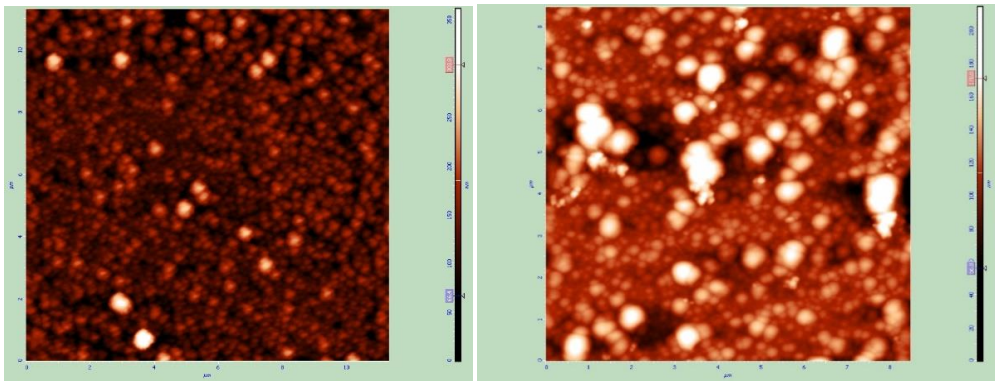

Figure 9: AFM images of soft vesicles formed from 1 (46.32 mM) in DMSO-water (2:1 v/v)

4.2.5.4 X-ray diffraction studies

The bilayer membrane morphology is supported by X-ray diffraction studies of the self-assemblies of 1 in DMSO-water (1% w/v, 2:1 v/v) where a sharp peak at 2□□= 4.04° was observed that corresponds to a d spacing of 2.24 nm (Figure 10).

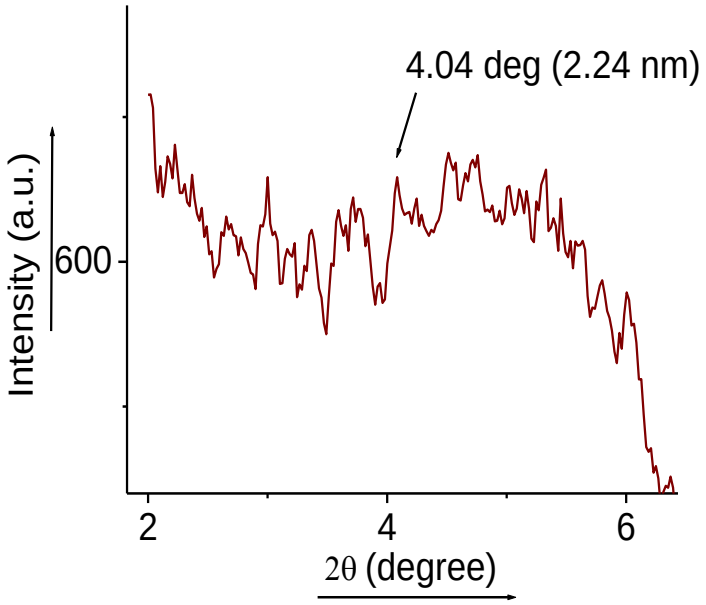

Figure 10: X-ray diffraction studies of the self-assemblies of **1** (1% w/v) in DMSO-water (2:1 v/v)

4.2.5.5 ATR studies

H-bonding involving the carboxyl groups in addition to the dispersion interactions by the macrocyclic diterpenoid backbones are likely to play a significant role for the self-assembly of the molecules. The stretching frequency of the 'C=O' group in the neat compound appeared at 1683 cm^{-1} whereas the 'C=O' stretching frequencies of the self-assemblies appeared at 1655 and 1658 cm^{-1} at 2% and 0.5% (w/v) in DMSO-water (2:1 v/v) respectively. The stretching frequency of the 'O-H' group in the self-assemblies appeared at 3394, and 3415 cm^{-1} in DMSO-water (2:1 v/v) at 2% and 0.5% (w/v) respectively (see Figure 11). The lowering of the "-C=O" stretching frequencies in the self-assemblies compared to the neat compound and lowering of

the "–O-H" stretching frequency with increasing concentration clearly indicated that the self-assemblies were stabilized by the intermolecular H-bonding among the molecules.

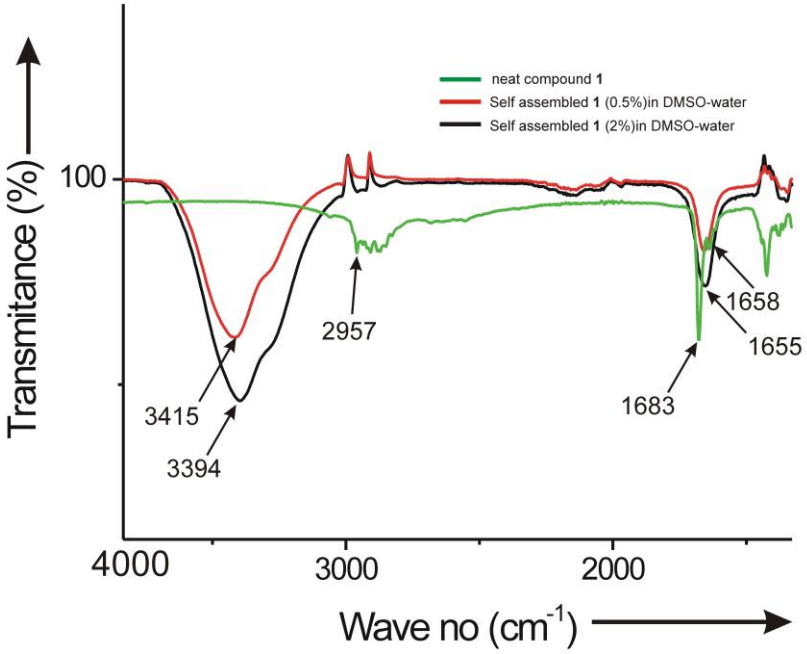

Figure 11: Overlay of the FTIR spectra of compound **1** (recorded in ATR mode).

4.2.5.6 DLS Studies

Dynamic Light Scattering (DLS) studies carried out with a dilute colloidal suspension of **1** (1.18% w/v) in ethanol-water (2:1 v/v) revealed polydisperse spherical self-assemblies with an average size of 200 nm with 15% of the spherical objects having diameter of 42 nm (see Figure 12). With increasing concentration of **1** to 1.6% w/v and 2.2% w/v, the average size of the self-assemblies increased to 465 nm and 523 nm respectively with a small fraction of the assemblies having micrometer diameters.

(a)

Results

		Size (r.nm):	% Intensity	Width (r.nm):
Z-Average (r.nm): 200.5	Peak 1:	242.7	82.7	19.79
PdI: 0.737	Peak 2:	42.28	17.3	2.203
Intercept: 0.777	Peak 3:	0.000	0.0	0.000

Result quality : Refer to quality report

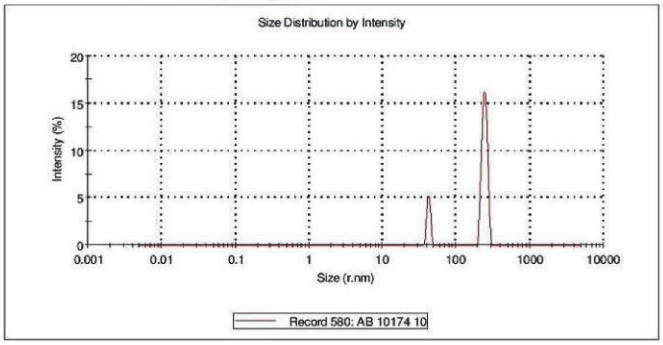

(b)

Results

		Size (r.nm):	% Intensity	Width (r.nm):
Z-Average (r.nm): 465.0	Peak 1:	405.8	76.5	46.07
PdI: 0.548	Peak 2:	66.09	14.3	2.855
Intercept: 0.606	Peak 3:	0.08319	8.0	0.001352

Result quality : Refer to quality report

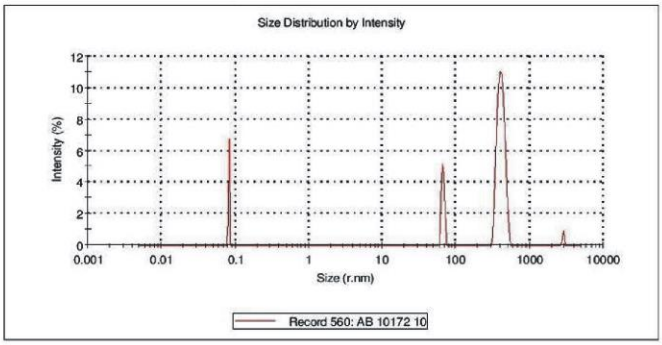

(c)

Results

		Size (r.nm):	% Intensity	Width (r.nm):
Z-Average (r.nm): 523.5	Peak 1:	231.1	79.7	8.933
PdI: 0.982	Peak 2:	72.29	14.2	1.751
Intercept: 0.932	Peak 3:	3.884	6.1	0.03231

Result quality : Refer to quality report

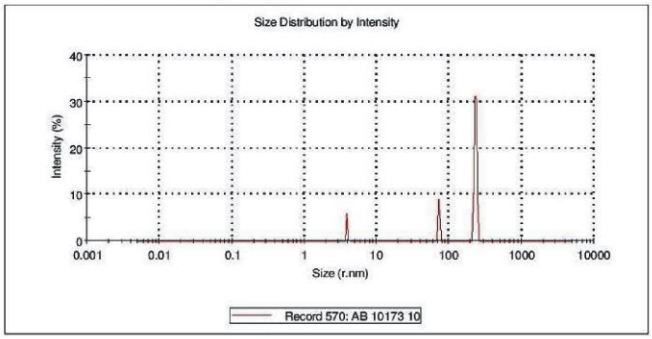

Figure 12: DLS studies of self-assembled **1** in ethanol-water (2:1, v/v): (a) 1.6% (b) 1.8% (c) 2.2%

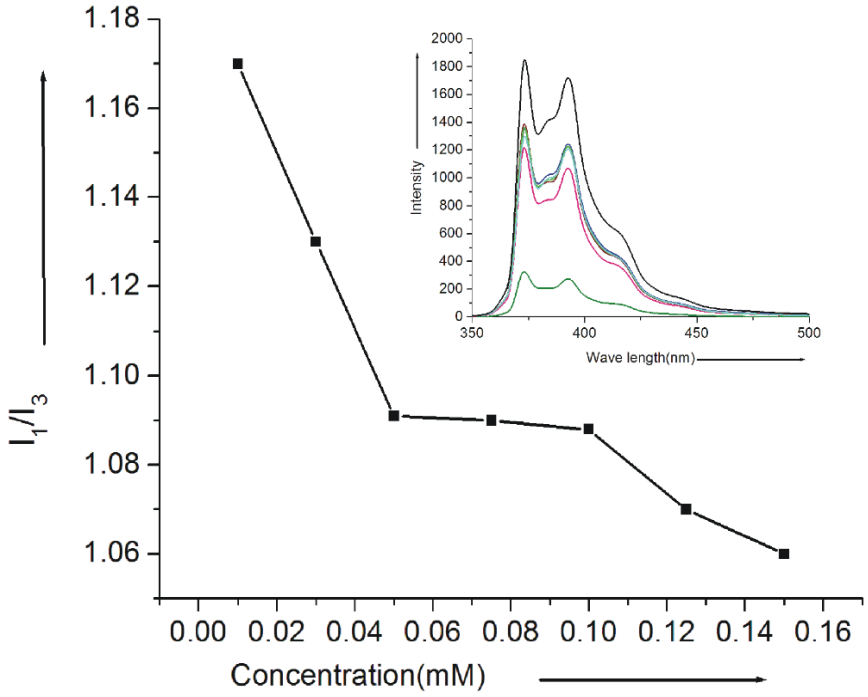

Figure 13 Variation of I_1/I_3 in the emission spectra of pyrene (fixed concentration = 10^{-6} M) encapsulated in **1** solutions of varying concentration, inset: emission spectra of pyrene in aqueous binary solvent mixture in presence of various concentration of **1**.

4.2.5.7 Determination of CVC by Fluorescence Spectroscopy using Pyrene as a probe:

Vesicular self-assemblies of amphiphiles in aqueous medium are formed above a critical concentration of the amphiphiles known as critical vesicular concentration (cvc). By using pyrene as a fluorescence probe cvc was determined to be 0.05 mM in DMSO-water (1:9 v/v, Figure 13).

The emission-intensities of the first (I1) and third (I3) vibronic peaks of pyrene are sensitive to the polarity of the microenvironment. Hence, the vesicular self-assembly of 1 was monitored by using pyrene as a hydrophobic probe. The I_1/I_3 ratio of pyrene, encapsulated in aqueous binary solvent mixture of 1, gradually decreased with increasing concentration of 1 until it reached a platue at the I_1/I_3 value of 1.09.

This is probably due to a hydrophobic microenvironment provided by self-assembled **1** beyond a critical concentration (0.05 mM) and the probe is located inside the self-assembly.

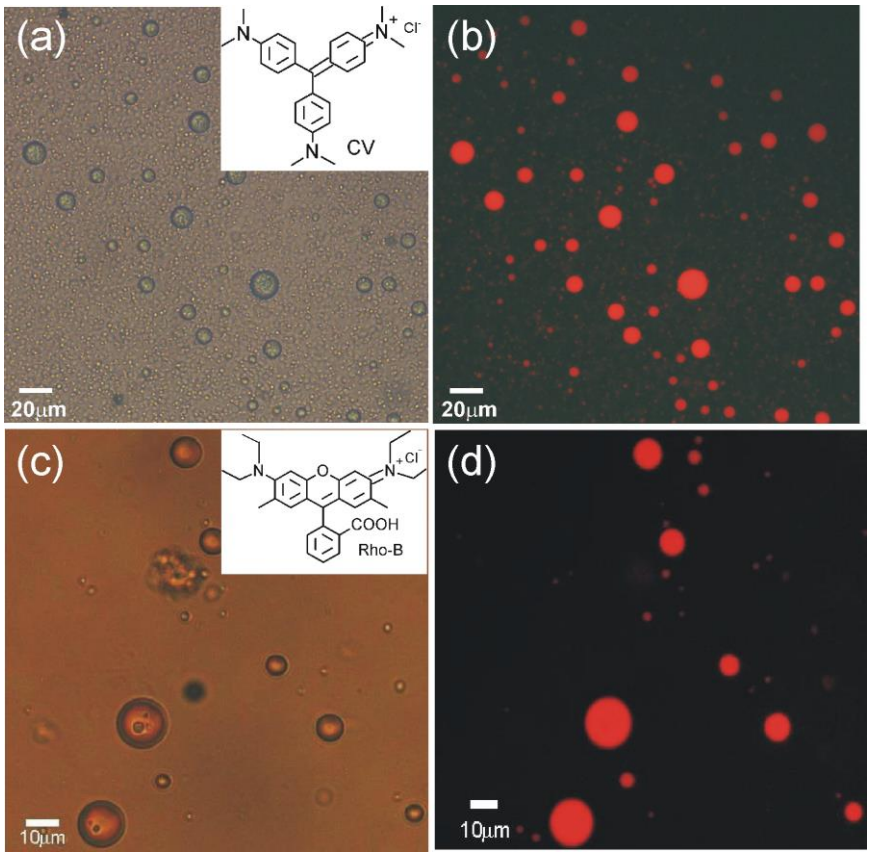

Figure 14: Epifluorescence microscopy images of self- assembled crotocembraneic acid **1** (46.32 mM) in DMSO-water (2:1 v/v) (a,b) containing crystal violet (0.463 mM), (c,d) containing rhodamine B (0.463 mM) (a,c) bright-field images, (b,d) fluorescent images.

4.2.6 Application of the self-assembly of Crotocembraneic acid

Development of biocompatible nano carriers has been an emerging area of research for efficient and targeted drug delivery with an aim to minimize the serious side-effects in chemotherapy.[21,22,23,24] Entrapment of drugs inside the self-assemblies and their subsequent release are integral parts for the demonstration of self-assembled ursolic acid as carriers. These studies with model fluorophore compounds as well as the anticancer drug doxorubicin are discussed in the following sections

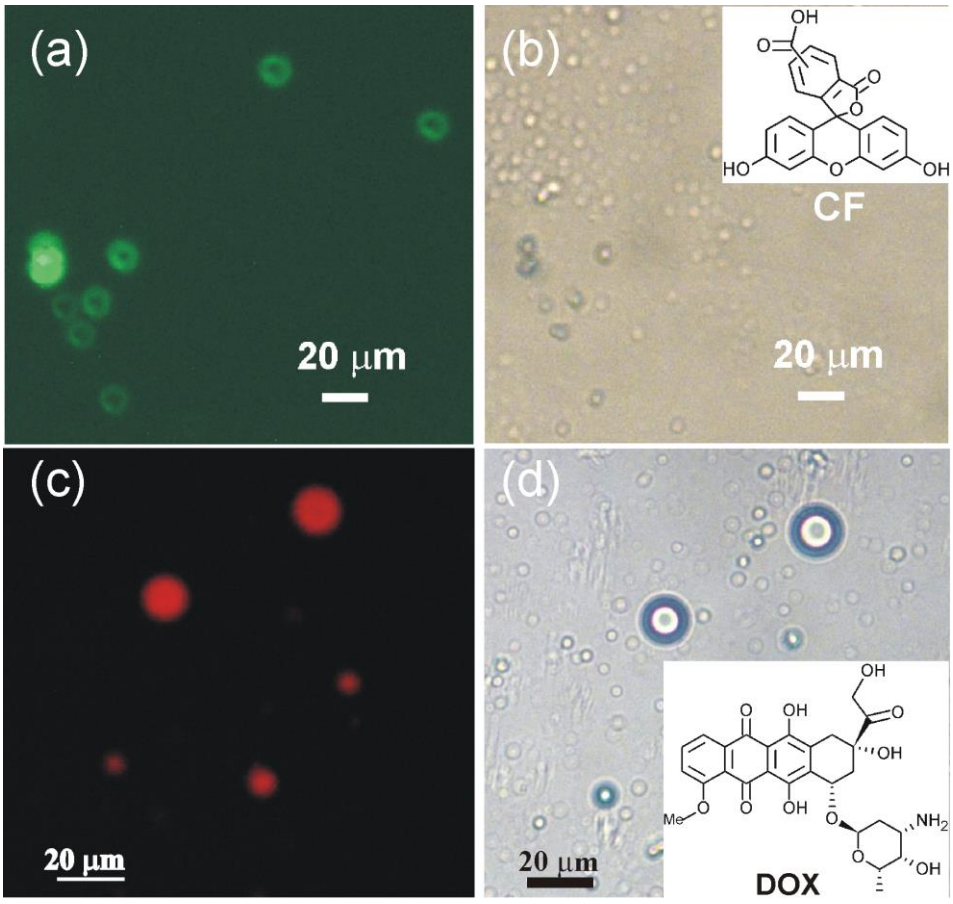

Figure 15: Epifluorescent microscopy images of (a,b) self-assembled **1** (26.0 mM) in DMSO-water (2:1 v/v) containing CF (0.26 mM); (c,d) self-assembled **1** (46.32 mM) in DMSO-water (2:1 v/v) containing doxorubicin (0.46 mM). (a,c) Fluorescent images, (b,d) bright-field image

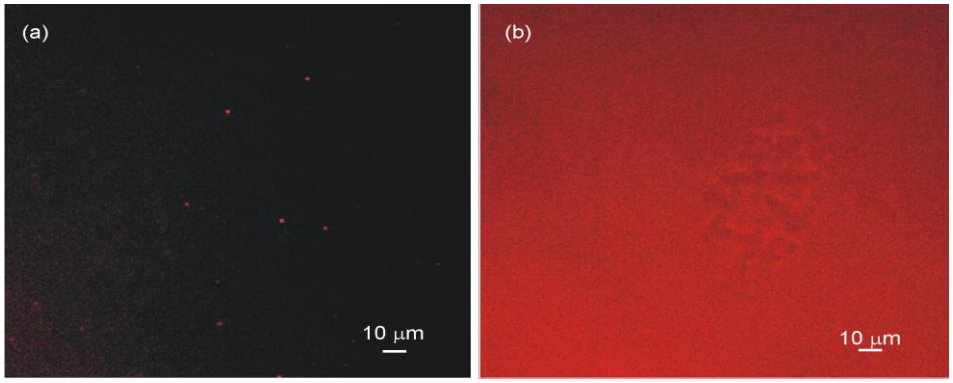

Figure 16: Optical microscopy images of (a) rhodamine B (0.46 mM) entrapped vesicles via self-assembly of crotocembraneic acid 1 (46.30 mM) and (b) after 20 min. of the addition of Triton-X-100 (0.46 mM) into the rhodamine B entrapped vesicular self-assembly of crotocembraneic acid 1 (a,b) under fluorescence light.

4.2.6.1 Study of entrapment and release of fluorophores including anticancer drug doxorubicin

Vesicular self-assemblies of average size smaller than 10 μm are an attractive choice for targeted drug delivery through blood capillaries.[12] Whether the vesicular self-assemblies of **1** are capable of entrapping guest molecules inside, we examined the entrapment of the cationic fluorophores crystal violet (CV) and rhodamine B (Rho-B) and an anionic fluorophore 5,6 carboxy-fluorescein (CF). Interestingly, both the cationic fluorophores as well as the anionic fluorophore were entrapped inside the vesicular self-assemblies of **1** (Figure 14,15). For example, when a hot solution of crotocembraneic acid **1** (46.32 mM) in DMSO-water (2:1 v/v) containing CV (0.463 mm) was cooled at room temperature and examined by epifluorescence microscopy, bright fluorescence was observed inside the spheres (Figure 14 a,b). Similarly, bright fluorescence of Rho-B was also entrapped inside the vesicular self-assemblies of **1** under identical condition (Figure 14 c,d). When a hot solution of **1** (26.0 mM) in DMSO-water (2:1 v/v) containing the anionic fluorophore CF (0.26 mM) was cooled at room temperature and examined by epifluorescence microscopy, slow entrapment of fluorophores were observed (Figure 15 a,b). The increased intensity of the fluorescence at the periphery indicated slow entrapment of the fluorophores inside the vesicles. All these studies also supported the vesicular nature of the spherical self-assemblies. To verify the entrapment of fluorophores inside the vesicular self-assemblies, we treated the Rho-B (0.46 mM) entrapped spherical self-assemblies of 1 (46 mM) with a small amount of triton X-100 (0.46 mM). Lysis of the spherical self-assemblies with concomitant release of the fluorophores confirmed their vesicular nature (see Figure 16).

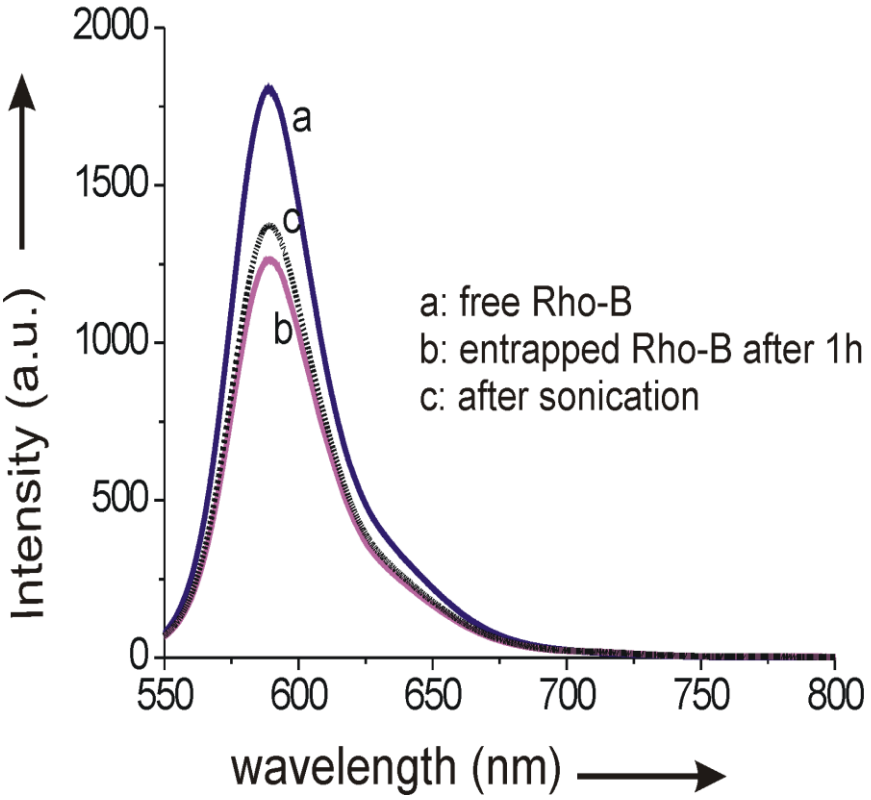

Figure 17: Fluorescence emission spectra (λ_{ex} = 510 nm) of Rho-B under different experimental conditions showing the effect of entrapment by vesicular self-assemblies and partial release by sonication.

Inspired by these observations, we tested the entrapment of the anticancer drug doxorubicin. When a hot solution of 1 (46.32 mM) in DMSO-water (2:1 v/v) containing doxorubicin (0.46 mM) was cooled at room temperature and examined under epifluorescence microscopy after 3 h, bright fluorescence from inside the vesicles confirmed the entrapment of doxorubicin inside the vesicular self-assemblies of 1 (Figure 15 c,d). Fluorescence quenching during entrapment of the fluorophores confirmed fluorophore entrapment inside the vesicles (Figure 17). Partial release of the entrapped fluorophores by sonication was also evident from fluorescence emission studies (Figure 17c).

4.3 Conclusion

In conclusion, we have reported the formation of vesicular self-assemblies of a naturally occurring macrocyclic diterpenoid crotocembraneic acid in aqueous media yielding vesicular self-assemblies. According to our knowledge, this is the first report of the formation of vesicular self-assemblies of a diterpenoid. Evidence for the formation of a bilayer vesicular structure has been obtained from HRTEM and X-ray diffraction studies. Thus crotocembraneic acid joins the rare class of macrocyclic natural products yielding vesicular self-assemblies in aqueous binary solvent mixtures. Entrapment of both cationic as well as anionic fluorophores including the anticancer drug doxorubicin inside the vesicles has also been demonstrated. The renewable nature of the diterpenoid and the simplicity of the methods of self-assembly and drug entrapment described here makes our strategy applicable to other naturally occurring diterpenoids some of which are under investigations in our laboratory and will be reported in due course.

4.4 Experimental Section

Methods of sample preparartion

Same as chapter 3.

Drug entrapment studies:

A hot solution of 1 in DMSO/water (2:1) was mixed with a solution of doxorubicin in water (0.46 mM, 0.025 mL) and the reddish mixture was allowed to 14 cool at room temperature and examined by epifluorescence microscopy after 3 h. Reddish fluorescence inside the vesicles confirmed the drug entrapment (Figure 6).

.

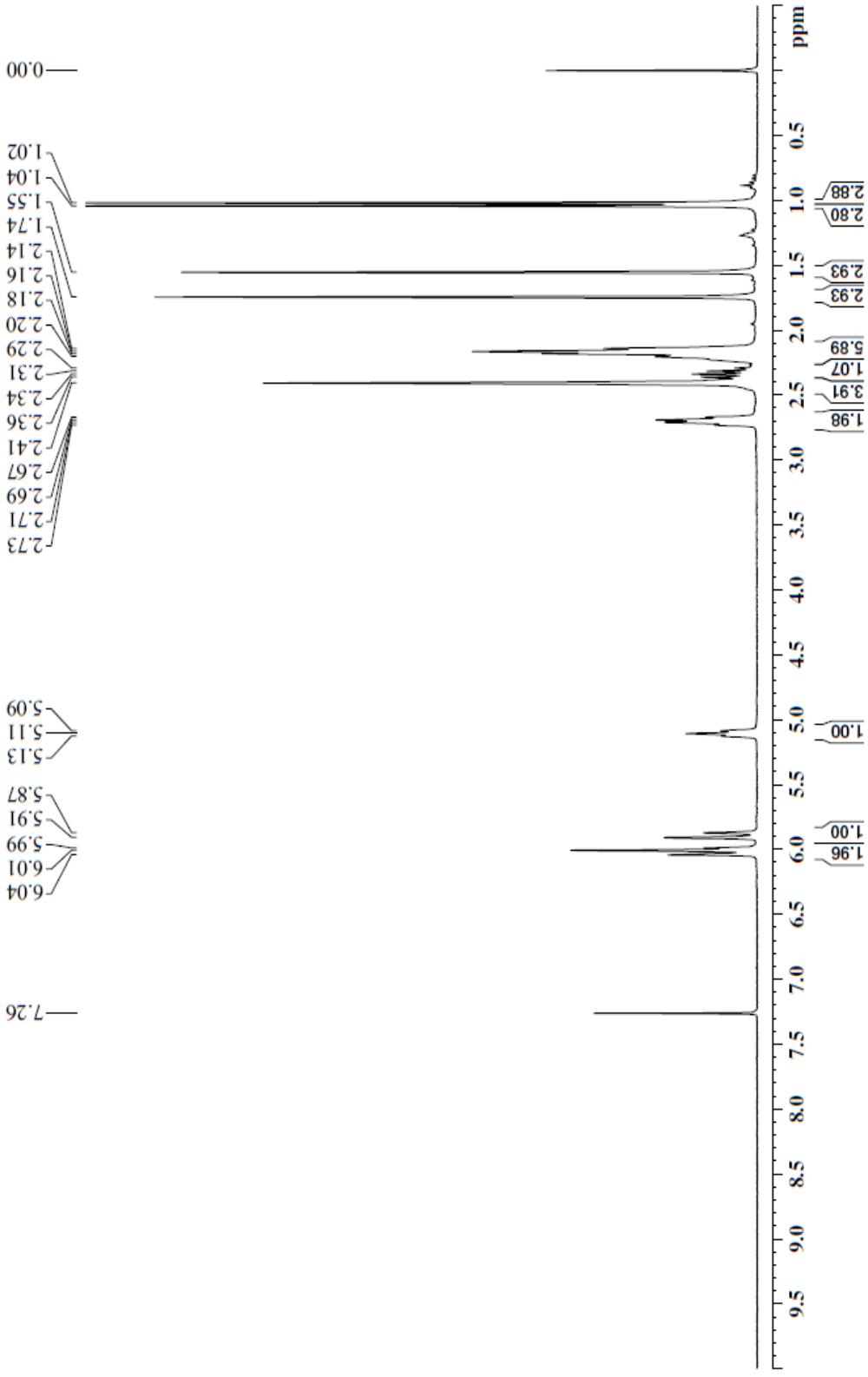

Figure 18: ^{1}H NMR ($CDCl_3$) of crotocembraneic acid (1)

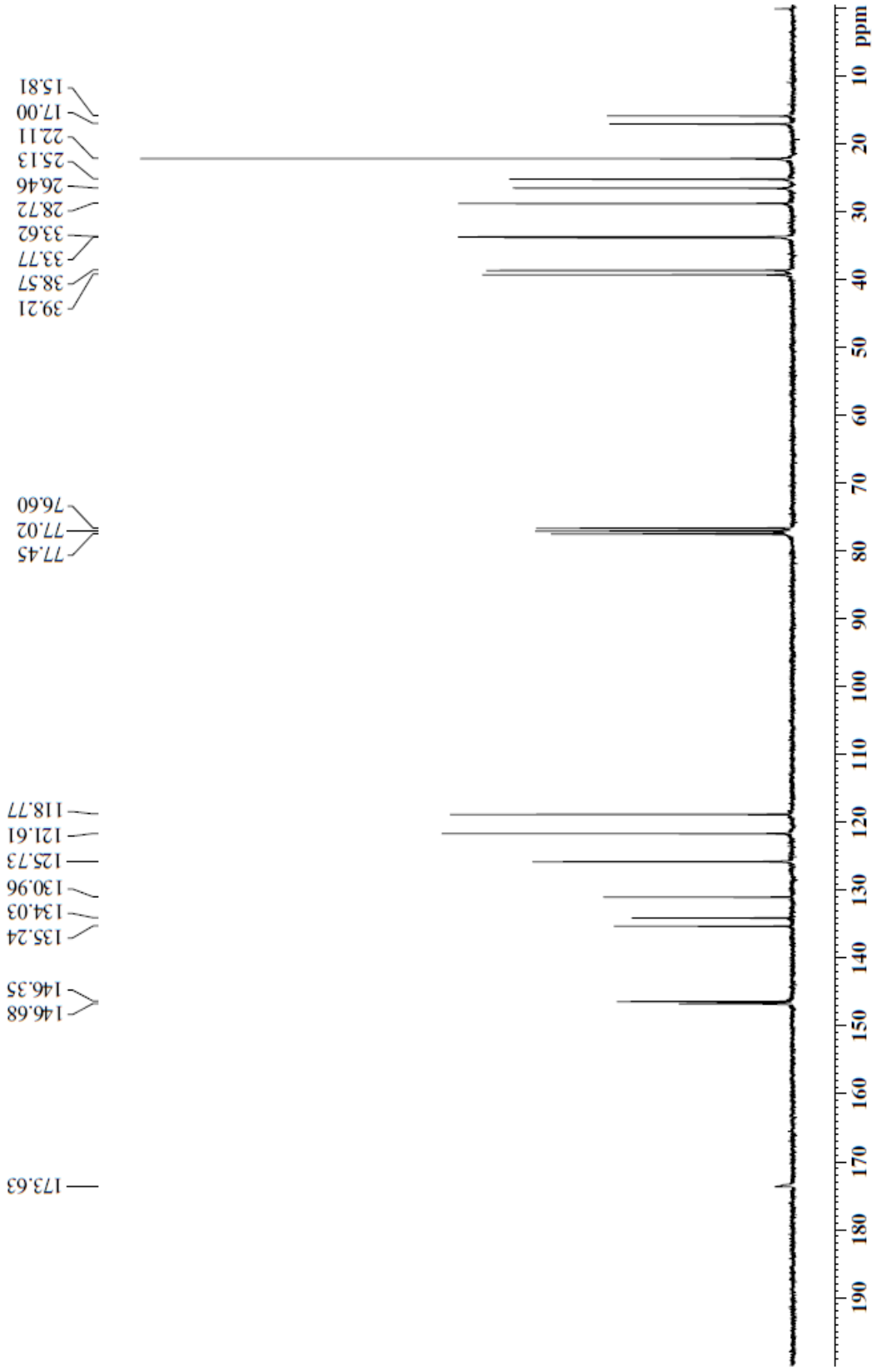

Figure 19: ^{13}C NMR ($CDCl_3$) of crotocembraneic acid (1)

4.5 References

1 (a) A. Sorrenti, O. Illa, R. M. Ortuno, *Chem. Soc. Rev.* **2013,** *42*, 8200; (b) C. A. E. Hauser, S. Zhang, *Nature* **2010**, 468, 516; (c) N. Amdursky, M. Molotskii, E. Gazit, G. Rosenman, *J. Am. Chem. Soc.* **2010**, *132*, 15632.

2 S. Bhattacharya, S.K. Samanta, *Chem. Rev.* **2016**, *116*, 11967−12028.

3 (a) E. Busseron, Y. Ruff, E. Moulin, N. Giuseppone, *Nanoscale* **2013**, **5**, 7098; (b) H.-B. Yao, H.-Y. Fang, X.-H. Wang, S.-H. Yu, *Chem. Soc. Rev.* **2011**,*40*, 3764; (c) M. Grzelczak, J. Vermant, E. M. Furst, L. M. Liz-Marza´n, *ACS Nano* **2010**, *4*, 3591.

4 (a) E. Carretti, M. Bonini, L. Dei, B.H. Berrie, L.V. Angelova, P. Baglioni and R.G.Weiss, *Acc. Chem. Res*. **2010**, *43*, 751; (b) S. S. Babu, V. K. Praveen, A. Ajayaghosh, *Chem. Rev.* **2014**, *114*, 1973; (c) M. Suzuki and K. Hanabusa, *Chem. Soc. Rev.* **2009**, *38*, 967; (d) M. George and R.G. Weiss, *Acc. Chem. Res.* **2006**, *39*, 489; (e) R.G. Weiss, P. Terech, in : Molecular Gels: Materials with Self-Assembled Fibrillar Networks; Springer: Dordrecht, **2006**.

5 (a) A. Ajayaghosh, V. K. Praveen, *Acc. Chem. Res.* **2007,** *40*, 644; (b) A. Ajayaghosh, R. Varghese, S. Mahesh, V. K. Praveen, *Angew. Chem. Int. Ed.* **2006**, *45*, 7729; (c) T. Shimizu, M. Masuda, H. Minamikawa, *Chem. Rev.* **2005**, *105*, 1401; (d) A. Ajayaghosh, R. Varghese, S. Mahesh, V. K. Praveen, *Angew. Chem. Int. Ed.* **2006,** *45*, 3261-3263.

6 B.G. Bag, R. Majumdar, *Chem. Rec.* **2017**, DOI: 10.1002/tcr.201600123

7 (a) P. Moitra, K. Kumar, P. Kondaiah, S. Bhattacharya, *Angew. Chem. Int. Ed.* **2014**, *53*, 1113; (b) S. K. Misra, P. Kondaiah, S. Bhattacharya, C. N. R.

Rao, *Small* **2012**, *8*, 131; (c) S. K. Misra, P. Moitra, B. S. Chhikara, P. Kondaiah, S. Bhattacharya, *J. Mater. Chem.* **2012,** *22*, 7985.

8 (a) A. Friggeri, B. L. Feringa, J. van Esch, *J. Controlled Release* **2004**, *97*, 241; (b) Z. Yang, G. Liang, L. Wang, B. Xu, *J. Am. Chem. Soc.* **2006,** *128*, 3038; (c) Z. Yang, H. W. Gu, D. G. Fu, P. Gao, K. J. K. Lam, B. Xu, *Adv. Mater.* **2004**, *16*, 1440; (d) Z. Yang, B. Xu, *Chem. Commun.* **2004**, 2424; (e) K. J. C. van Bommel, M. C. A. Stuart, B. L. Feringa, J. van Esch, *Org. Biomol. Chem.* **2005**, *3*, 2917.

9 J.M. Suh, S.J. Bae, B. Jeong, *Adv. Mater.* **2005**, *17*, 118-120.

10 (a) S. Dutta, T. Kar, D. Mandal, P. K. Das, *Langmuir* **2013**, *29*, 316; (b) P. K. Vemula, J. Li, G. John, *J. Am. Chem. Soc.* **2006**, *128*, 8932; (c) P.K. Vemula, G. John, *Chem. Commun.* **2006**, 2218; (d) N. Sreenivasachary, J.-M. Lehn, *Proc. Natl. Acad. Sci. U.S.A.* **2005**, *102*, 5938.

11 Y. Jeong, M. K. Joo, Y. S. Sohn, B. Jeong, *Adv. Mater.* **2007**, *19*, 3947–3950

12 M. Antonietti, S. Foerster, *Adv. Mater.* **2003**, *15*, 1323-1333.

13 B. Kamm, *Angew. Chem. Int. Ed*. **2007**, *46*, 5056 – 5058.

14 (a) B.G. Bag, K. Paul, *Asian J. Org. Chem.* **2012**, *1*, 150; (b) M. Delample, F. J´erˆome, J. Barrault, J.-P. Douliez, *Green Chem.*, **2011**, *13*, 64; (c) B. Novales, L. Navailles, M. Axelos, F. Nallet and J.-P. Douliez, *Langmuir*, **2008**, *24*, 62; (d) B. G. Bag, S. Das, S. N. Hasan, A. C. Barai, *RSC Adv*. **2017**, *7*, 18136.

15 S. Dinda, M. Ghosh, P.K. Das, *Langmuir* **2016**, *32*, 6701−6712

16 B. G. Bag, R. Majumdar, *RSC Adv.* **2014**, *4*, 53327-53334.

17 B.G. Bag, S.S. Dash, *Langmuir* **2015,** *31*, 13664-13672.

18 B.G. Bag, S.S. Dash, *Nanoscale* **2011**, *3*, 4564-4566.

19 B. G. Bag, R. Majumdar, *RSC Adv.* **2012**, *2*, 8623 –8626.

20 B. G. Bag, A. C. Barai, K. Wijesekera, P. Kittakoop., *ChemistrySelect*, **2017**, *2*, 4969.

21 (a) R. T. Skeel and S. N. Khleif, *Handbook of Cancer Chemotherapy*, **2011**, 8, 1; (b) L. Williams and Wilkins, *Handbook of Cancer Chemotherapy*, **2011**, *8*, 45.

22 B. Tian, X. Tao, T. Ren, Y. Weng, X. Lin, Y. Zhang, X. Tang, *J. Mater. Chem.*, **2012**, *22*, 17404.

23 P. Moitra, K. Kumar, P. Kondaiah, S. Bhattacharya, *Angew. Chem., Int. Ed.* **2014**, *53*, 1113.

24 A. Ali, M. Kamra, A. Bhan, S. S. Mandal, S. Bhattacharya, *Dalton Trans.*, **2016**, *45*, 9345.